FEMS Yeast Research, 19, 2019, foz042

https://doi.org/10.1093/femsyr/foz042
Advance Access Publication Date: 20 June 2019
Research Article

RESEARCH ARTICLE

The synthetic cannabinoid JWH-018 modulates *Saccharomyces cerevisiae* energetic metabolism

Carla Ferreira[1,2,3], Joana Couceiro[1,2], Carlos Família[1,2], Carolina Jardim[4,5], Pedro Antas[6], Cláudia N Santos[4,5,6], Tiago F Outeiro[6,7,8,9], Sandra Tenreiro[6] and Alexandre Quintas[1,2,*,†]

[1]Molecular Pathology and Forensic Biochemistry Laboratory, Centro de Investigação Interdisciplinar Egas Moniz, P-2825-084 Caparica, Portugal, [2]Laboratório de Ciências Forenses e Psicológicas Egas Moniz, Campus Universitário – Quinta da Granja, Monte de Caparica, P-2825-084 Caparica, Portugal, [3]Faculty of Medicine of Porto University, Al. Prof. Hernâni Monteiro, P-4200–319 Porto, Portugal, [4]Instituto de Biologia Experimental e Tecnológica, Apartado 12, P-2780–901 Oeiras, Portugal, [5]Instituto de Tecnologia Química e Biológica, Universidade Nova de Lisboa, Av. da República, P-2780-157 Oeiras, Portugal, [6]CEDOC – Chronic Diseases Research Center, Faculdade de Ciências Médicas, Universidade Nova de Lisboa, P-1150-082 Lisboa, Portugal, [7]Department of Experimental Neurodegeneration, Center for Nanoscale Microscopy and Molecular Physiology of the Brain, University Medical Center Göttingen, Waldweg 33. Göttingen P37073, Germany, [8]Institute of Neuroscience, Medical School, Newcastle University, Framlington Place, Newcastle Upon Tyne P-NE1 7RU, UK and [9]Max Planck Institute for Experimental Medicine, Hermann Rein Street 3. P-37075 Göttingen, Germany

[*]**Corresponding author:** Molecular Pathology and Forensic Biochemistry Laboratory, Centro de Investigação Interdisciplinar Egas Moniz. Tel: +351 212946769; E-mail: aquintas@egasmoniz.edu.pt

One sentence summary: Present work implemented *S. cerevisiae* model to understand the impact of JWH-018 on molecular and cellular levels. The results showed that JWH-018 improves cell fitness by modulating glycolytic levels.

Editor: Cristina Mazzoni

[†]Alexandre Quintas, http://orcid.org/0000-0002-5188-0453

ABSTRACT

Synthetic cannabinoids are a group of novel psychoactive substances with similar properties to Δ^9-THC. Among the vast number of synthetic cannabinoids, designed to be tested in clinical trials, JWH-018 was the first novel psychoactive substance found in the recreational drug marketplace. The consumption of JWH-018 shows typical effects of CB1 agonists including sedation, cognitive dysfunction, tachycardia, postural hypotension, dry mouth, ataxia and psychotropic effects, but appeared to be more potent than Δ^9-THC. However, studies on human cells have shown that JWH-018 toxicity depends on the cellular line used. Despite these studies, the underlying molecular mechanisms to JWH-018 action has not been clarified yet. To understand the impact of JWH-018 at molecular and cellular level, we used *Saccharomyces cerevisiae* as a model. The results showed an increase in yeast growth rate in the presence of this synthetic cannabinoid due to an enhancement in the glycolytic flux at expense of a decrease in pentose phosphate pathway, judging by 2D-Gel proteomic

Received: 17 January 2019; **Accepted:** 18 June 2019

analysis, qRT-PCR experiments and ATP measurements. Overall, our results provide insights into molecular mechanisms of JWH-018 action, also indicating that *Saccharomyces cerevisiae* is a good model to study synthetic cannabinoids.

Keywords: JWH-018; proteomics; *Saccharomyces cerevisiae*; Synthetic cannabinoids; toxicity assays

INTRODUCTION

The medical use of cannabis predates history, finding its first record in ancient China 4700 years ago (Zuardi 2006). The main psychoactive component of cannabis is Δ^9-tetrahydrocannabinol (Δ^9-THC) which was first isolated by Gaoni and Mechoulam in 1964 (Gaoni and Mechoulam 1964). During the 1980s, it was found that Δ^9-THC action mechanism is receptor-mediated by the cannabinoid receptors 1 (CB1) and 2 (CB2) (Devane *et al.* 1988). This finding was supported by the observation of adenylate cyclase inhibition by natural and synthetic cannabinoids (SC) (Askew and Ho 1974; Lee and Phillis 1977; Reich *et al.* 1982; Li and Ng 1984; Heepe and Starke 1985; Howlett, Qualy and Khachatrian 1986). The United Nations acts of 1961 and 1971 imposed the control of narcotics and psychotropic substances. Due to these restrictions in the early 1980s, Pfizer© and Lilly© developed SC mimicking the effects of Δ^9-THC (McCarthy and Borison 1981). Subsequently, many other cannabinoids-like molecules have been synthetised aiming therapeutic uses (Howlett *et al.* 2002). However, just Nabilone was approved by FDA (Urits *et al.* 2019).

Currently, there are several studies suggesting the protective effects of natural and SC (Shohami, Novikov and Mechoulam 1993; Bar-Joseph *et al.* 1994; Vered *et al.* 1994; Shohami *et al.* 1997; Shen and Thayer 1998; Nagayama *et al.* 1999; Fernández-López *et al.* 2006; Koch *et al.* 2011; Pinar-Sueiro *et al.* 2013). Actually, WIN 55,212–2 exerts a neuroprotective effect in hippocampal neurons exposed to low extracellular magnesium concentrations, which induces cell death (Shen and Thayer 1998), and in cortical neurons under hypoxia and glucose deprivation (Nagayama *et al.* 1999). Moreover, HU-211 reduces neuronal damage in animal models of global ischaemia (Bar-Joseph *et al.* 1994; Vered *et al.* 1994; Fernández-López *et al.* 2006; Pinar-Sueiro *et al.* 2013). The same HU-211 has shown to improve motor and memory functions after a traumatic brain injury by reducing the oedema and blood–brain barrier breakdown (Shohami, Novikov and Mechoulam 1993; Shohami *et al.* 1997). Overall, cannabinoids seem to play a protective role in neurodegeneration improving muscle spasticity (Petro and Ellenberger 1981) and tremor (Clifford 1983), attenuating the symptoms of Parkinson's disease and multiple sclerosis. These effects seem to be related with cannabinoids' ability to reduce inflammatory mediators (Gruol *et al.* 1998; Puffenbarger, Boothe and Cabral 2000; Smith, Terminelli and Denhardt 2000; Koch *et al.* 2011). Additionally, several studies have been suggesting that cannabinoids have anti-cancer properties as exemplified by the suppressive effect of SC JWH-133 and WIN-55,212–2 in breast tumour (Qamri *et al.* 2009).

Despite the potential therapeutic of the previously described cannabinoids, there are many clinical reports pointing negative impacts of these molecules (Robinson *et al.* 2007; Crane 2013; Meijer, Russo and Adhvaryu 2014; Irie *et al.* 2015; Nurmedov *et al.* 2015; Rojek *et al.* 2017; Fantegrossi, Wilson and Berquist 2018). A magnetic resonance imaging study showed a grey matter density reduction in SC' abusers (Nurmedov *et al.* 2015). Another study has shown impairment of memory and hippocampal activity induced by HU-210 due to abnormalities in hippocampal cell firing (Robinson *et al.* 2007). At molecular level, MAM-2201 has been proven to suppress glutamate release in humans CB1-expressing synapses, which, according to the authors, may contribute to some of the symptoms of SC intoxication including impairments in cerebellum-dependent motor coordination and motor learning (Irie *et al.* 2015). In fact, consumers of SC have been given entry in hospital's emergency room with psychosis (Fantegrossi, Wilson and Berquist 2018), seizures (Malyshevskaya *et al.* 2017) and auto-inflicting injuries (Meijer, Russo and Adhvaryu 2014). Suicide (Crane 2013) and fatal cases (Rojek *et al.* 2017) were also reported. Despite the several contraindications described in the literature, a risk assessment study with JWH-018 was conducted in humans for the first time. This pilot study was sufficient to exclude this molecule for further consideration of therapeutic use (Theunissen *et al.* 2018). Also, other researches on human cells have shown that JWH-018 toxicity depends on the cellular line used, presenting no toxicity to hepatomas (Hep-G2) and neuroblastomas (SY-SH5) and moderate toxicity to human breast cells (MCF-7) and buccal cells (TR146) (Koller *et al.* 2013; Couceiro *et al.* 2016).

Taken together, the previous studies and clinical reports suggest the need of additional research to get the full picture of cannabinoids' effects in human health and disease. To further investigate the molecular mechanism of SC and understand the metabolic implications of these substances, a simplified model is required.

Saccharomyces cerevisiae shares highly conserved molecular and cellular mechanisms with human cells and simplifies the approach to understand cells fundamental biochemistry in a variety of different conditions. Yeast has been proven an invaluable model to study the fundamental molecular mechanisms involved in several human diseases (Tenreiro and Outeiro 2010). Moreover, it has also been used to study the toxicity of synthetic cathinones, pharmaceutical drugs and environmental pollutants impact (Hu *et al.* 2003; Schmitt *et al.* 2004; Tenreiro and Outeiro 2010; dos Santos *et al.* 2012; Tenreiro *et al.* 2013; Ferreira *et al.* 2019). Actually, the rapid growth associated to its high degree of conservation with human cellular pathways makes yeast a very interesting model to study SC. Therefore, the present study used *S. cerevisiae* to understand the impact of JWH-018 at cellular and molecular level. JWH-018, a SC synthetised by John W Huffman in 1994 as an antinociceptive, was the first legal alternative to cannabis used for recreational purposes and since then classified as a novel psychoactive substance (Lainton *et al.* 1995; Wiley *et al.* 1998). The present work used *S. cerevisiae* as a model to understand the cellular and molecular mechanisms of JWH-018 aiming to support target studies in more complex systems.

MATERIAL AND METHODS

Reagents

The YNB–Difco Yeast Nitrogen Base without Amino Acids, agar (Bacto) and peptone (Bacto) were obtained from Quilaban. The amino acids were acquired as a mixture from MPBiomedicals. Glucose, tris-hydrochloride (Tris-HCl), sodium chloride (NaCl) and sodium dodecil sulfate (SDS) were acquired from Panreac. Bradford reagent (Bio-Rad Protein Assay Dye Reagent Concentrate), bovine serum albumin (BSA), ReadyPrep 2-D

kit, urea, IPG strips pH 3–10 NL, iodoacetamide, protein marker (Precision Plus Protein™ Standards Dual Colour) and Flamingo™ Fluorescent Gel Stain were acquired from Bio-Rad. Thiourea was obtained from Millipore. CHAPS from BioChemica, ampholytes (pH 3–10) from GE Healthcare, dithiothreitol (DTT) from Amresco, and glycerol obtained from Scharlau.

Tested compounds

The synthetic cannabinoid JWH-018 [(1-pentyl-1H-indol-3-yl)-1-naphthalenyl-methanone] was acquired from Lipomed AG Switzerland in the form of powder with a purity greater than 98.5%. Stock solutions of this compound were prepared in 100% DMSO in different concentrations: 0.25 mM, 2.50 mM, 12.50 mM, 18.75 mM and 25.00 mM.

Cell culture

The study was performed using *S. cerevisiae* cells (BY4741 MATa; his3Δ1; leu2Δ0; met15Δ0; ura3Δ0 obtained from Euroscarf collection (Frankfurt, Germany)). Yeast cells were pregrown in YNB (Yeast Nitrogen Base without Amino Acids 0.67%, Glucose 2%, Required amino acids) liquid media at 30°C, with orbital agitation (200 rpm) for 6 hours. After 6 hours, the optical density at 600 nm (OD_{600nm}) was measured and cultures were diluted to a standardised $OD_{600\,nm} = 2 \times 10^{-3}$ ($\sim 1.67 \times 10^5$ cells/mL) in the same medium. After 19 hours, new cultures were prepared to have an initial standardised $OD_{600nm} = 0.03$ (2.5×10^4 cells/mL) in the same medium, under the same conditions for 24 hours.

Toxicity experiments

The cytotoxic properties of JWH-018 were investigated through the evaluation of the cell growth kinetics, cell viability and spot assay in the presence of 1 μM, 10 μM, 50 μM, 75 μM and 100 μM of the SC. Growth analysis was monitored for 24 hours by a thermostatic microplate reader PowerWave XS (Biotek) at 30°C at 600 nm with readings every hour. The data were collected by Gene5 data analysis software. In order to count CFUs, several points were collected and diluted during yeast growth and were incubated for 2 days at 30°C on YPD agar plates (Yeast extract 1%, Peptone 2%, Glucose 2%, agar 2%).

Models for fitting toxicity experiments

Growth curves were fitted to the standard form of the logistic equation (Equation (1)) after subtraction of the minimum value, through growthcurver v.0.2.1 package for R v.3.5.0.

$$N_t = \frac{K}{1 + \left(\frac{K - N_0}{N_0}\right) e^{-rt}} \quad (1)$$

where r is the growth rate, N_0 is the initial population size and K the final biomass. The doubling time (t_d) value was computed from the growth rate (r) using the formula $Ln2/r$.

CFU data were analysed using the GraphPad prism software® v.4 (La Jolla, CA, USA) with the exponential growth equation, whose doubling time was calculated by this software.

Sampling and protein extraction for 2-D Electrophoresis

Three independent growth experiments were carried out to obtain cell replicates with 100μM of JWH-018 and without JWH-018 (control). Both samples were collected in the mid-exponential growth-phase. Cultures samples were centrifuged (12 100 g for 5 min at 4°C) and washed with cold distilled water. The cell pellets were immediately stored at –80°C until use. Cell pellets from the same culture condition were thawed on ice and pooled together by resuspension in lysis buffer (50 mM Tris-HCl, 150 mM NaCl pH 7.3) supplemented with protease inhibitor cocktail (Sigma). Briefly, cell lysis was carried out by consecutive steps of vortexing and ice cooling with an equal volume of glass beads (f = 425–600 mm). The mixture was centrifuged at 12 100 g at 4°C for 5 min to separate cell debris and glass beads from the supernatant, after which the cell pellets were disrupted again as described above. The resulting supernatant was mixed with the one obtained before, and the mixture was clarified by centrifugation at 12 100 g at 4°C for 5 min. Protein concentration of the resulting cell extracts was quantified using the Bio-Rad Protein Assay Dye Reagent Concentrate. Total protein (75 μg) was precipitated using the ReadyPrep 2-D (Bio-Rad), and the protein pellets were dissolved in 170μL of rehydration solution (7 M Urea; 2 M Thiourea; 2% w/v CHAPS; 0.5% ampholytes pH 3–10; 0.28% DTT; 0.002% bromophenol blue). The mixture was homogenised. All reagents used in this study were of analytical grade.

2-D Electrophoresis

Isoelectric focusing (IEF) was performed using the Protein i12 IEF cell (Bio rad), using IPG strips (11 cm Ready Strip, pH 3–10 NL; BioRad) which were rehydrated of 170μL of protein samples in rehydration solution for 17 hours before being transferred to the isoelectric system. IEF was carried out at 150 V for 10 min; 250 V for 20 min; 800 V for 2 hours; 1400 V for 1.75 hours; 3000 V for 2 hours; 6500 V for 1.86 hours and 8000 V for 2 hours. After the first dimension, the strips were equilibrated in two sequential 15 min steps in the adequate buffer (6 M Urea; 50 mM Tris-HCl, pH 8.8; 30% (v/v) glycerol; 2% (m/v) SDS; bromophenol blue) containing 65 mM DTT (step 1), or 135 mM iodoacetamide (step 2). The second dimension was performed using 11 cm SDS polyacrylamide (Criterion™ TGX™ precast gels 8–16%, Bio-Rad). In the second dimension were applied molecular weight standards (Precision Plus Protein™ Standards Dual Colour, Bio-Rad). Proteins were separated at 120 V. After the second-dimension run, protein spots were stained with fluorescent dye (Flamingo™ Fluorescent Gel Stain, Bio-Rad) according to the manufacturer's instructions. After destaining, the gels were washed two times and scanned in a laser imager with emission at 473 nm (FLA-5000 Imaging System).

Analysis of protein expression results from 2-DE

In total, three 2-DE gels for each experimental condition, corresponding to triplicates of biological samples per condition, were analysed. The images were analysed using Progenesis Same Spots software (Nonlinear Dynamics, Durham, NC, USA). Individual spot volumes were normalised against the total spot volumes for each gel. For each growth condition, the average value was compared by their normalized volume using one-way analysis of variance between-group testing. Statistically significant spots ($P < 0.05$) were selected for putative identification. This was performed by comparison with gels 2D in SWISS-2DPAGE (https://world-2dpage.expasy.org).

Interaction networks between proteins were obtained from STRING (http://string.embl.de/) (von Mering *et al.* 2007), a web-based resource containing a database that encompasses

known and predicted protein–protein interactions for 373 organisms, including *S. cerevisiae* and humans. Human proteins with sequence homologues that were found to be involved in the response to JWH-018 in *S. cerevisiae* were identified by BLASTP sequence homologuey searches at NCBI (http://www.ncbi.nlm.nih.gov/). Pathway queries for yeast and human proteins were performed at SGD (www.yeastgenome.org) and NCBI.

Quantitative Real-time -PCR (qRT-PCR)

RNA was extracted according to the manufacturer's instructions kit (E.Z.N.A. Yeast RNA Kit, OMEGA). The cDNA was synthesised from 500 ng of DNAse-treated total RNA using the SuperScript II Reverse Transcriptase (Invitrogen) following the supplier's recommendations. qRT-PCR was performed using LightCycler®480 SYBR Green I Master. The reaction mixture without template cDNA was run as a control. The expression was normalised to *PGK1*. PCR conditions used in the reaction were as follows: initial denaturation at 95°C for 10 s, followed by 45 cycles with the following cycling parameters – denaturation at 95°C for 10 s, annealing at 60°C for 10 s and elongation at 72°C for 30 s. Fold change was calculated using double delta Ct method. The data were expressed as mean ± standard error. Primers' sequences are indicated in Suplementary data.

ATP quantification

Three independent growth experiments were carried out to obtain cell replicates with 100μM of JWH-018 and without JWH-018 (control). The quantification of ATP was carried out using ATP Colorimetric/Fluorimetric assay kit from Sigma-Aldrich. Both samples were collected in the mid-exponential growth-phase. Three hundred microliters of cultures samples were centrifuged (12 100 g for 5 min at 4°C) and washed with cold distilled water. The cell pellets were immediately frozen in liquid nitrogen. After that, the cells were resuspended in ATP assay buffer and cell lysis was carried out by consecutive steps of vortexing and ice cooling with an equal volume of glass beads (f = 425–600 mm). The mixture was centrifuged at 12 100 g at 4°C for 1 min to separate cell debris and glass beads from the supernatant, after that, the ATP quantification was performed according to conditions described under colorimetric detection. In order to normalise the ATP values, protein quantification was performed using Bio-Rad protein assay dye reagent concentrate.

Statistical analysis

Linear mixed effects models were used to analyse the relationship between SC's concentration and each of the parameters resulting from the non-linear fit to the logistic equation, where repetitions nested within replicates were considered as random effects. Models were fitted through restricted maximum likelihood (RML) with the function lmer, provided by the package lmerTest v.3.0–1 for R v.3.5.1. Model estimates were summarised in tables using the sjt.lmer function provided by the sjPlot v.2.4.0 package for R v.3.5.1. *P*-values were computed through an analysis of variance of type III with the Kenward–Roger approximation for the degrees of freedom. Plots were made using ggplot2 v.3.0.0 package for R.

Student's *t*-test was used to analyse the differences in CFU viability assay, qRT-PCR results and ATP quantification.

RESULTS

Cytotoxicity assays

To investigate the effect of JWH-018, *S. cerevisiae* wild-type was exposed to growing concentrations of this SC. Cellular grow with 0, 1, 10, 50, 75 and 100 μM of JWH-018 was monitored by optical density at 600 nm during a time frame of 24 hours (Fig. 1A). Yeast growing rates in the presence of JWH-018 do not seem to be considerably different when compared to the control, suggesting the absence of an effect of this substance within the range of concentrations used. To further understand putative differences between yeast growth rates in the presence and absence of JWH-018, the curves were fitted to a logistic equation, which originates final biomass, growth rate (Fig. 1B) and the doubling time (Fig. 1C). Linear mixed effects models were used to statistically evaluate putative differences on growth rate (r), doubling time (t_d) and final biomass (K), with SC concentration. These models showed to be significantly different from the null model for concentrations equal or higher than 50 μM ($P < 0.05$). Actually, growth rate shows an estimated average value for 0 μM of JWH-018 of 0.5398 ± 0.0077. This value significantly increases by 0.0132 ± 0.0059, 0.0240 ± 0.0059 and 0.0265 ± 0.0058 for the concentrations 50 μM, 75 μM and 100 μM ($t(92.37) = 2.23$, $P = 0.026$; $t(92.37) = 4.04$, $P < 0.001$; $t(92.20) = 4.46$, $P < 0.001$). Consequently, it originates doubling time values of 1.2839 ± 0.0175 hours for concentration 0 μM, which decreases by 0.0287 ± 0.0134, 0.0521 ± 0.0134 and 0.0570 ± 0.0134 hours, for the concentrations of 50 μM, 75 μM and 100 μM, respectively. In opposite, the model developed to evaluate the effect of concentration on final biomass did not show significant differences between the absence and the presence of 100 μM of JWH-018. The non-linear analysis of the data shows differences in growth rate which were hidden in the initial picture.

To confirm the decrease on yeast duplication time in the presence of JWH-018 registered on the growth curves, CFU assays were performed (Fig. 2). The non-linear adjust shows that duplication time obtained was lower for cells in the presence of 50 μM of JWH-018 (Fig. 2), corroborating the results obtained in the analysis of the growth curves previously described (Fig. 1). However, after statistical analysis, the decrease in doubling time in the presence of 50μM of the SC was not significantly different from the culture without the compound.

S.cerevisiae proteome analysis

To grasp the molecular mechanisms underlying the increase in the growth rate of *S. cerevisiae* in the presence of JWH-018, a proteomic study was conducted. The concentration of JWH-018 chosen for this assay was 100 μM as it combines a higher effect on growth rate with the absence of toxicity. The proteome of *S. cerevisiae* in the absence and in the presence of 100 μM of JWH-018 was analysed in 2D electrophoresis gel system. Comparative and quantitative analyses of the 2D protein profiles were carried out using Progenesis SameSpots (Totallab, Reino Unido). In this study 2D gels triplicates for each of the *S. cerevisiae* cultures were analysed. The range of protein separation obtained by a 2DE was 10–250 kDa and 3–10 pH and 2181 protein spots were detected (Fig. 3). After a statistical analysis comparing yeast proteome in the absence and in the presence of JWH-018, eight proteins were found with statistically significant differences in their levels ($P < 0.05$). Fig. 3 shows the proteomic pattern of *S. cerevisiae* in the presence of JWH-018. One to eight marked spots show differences between the control and proteome with the

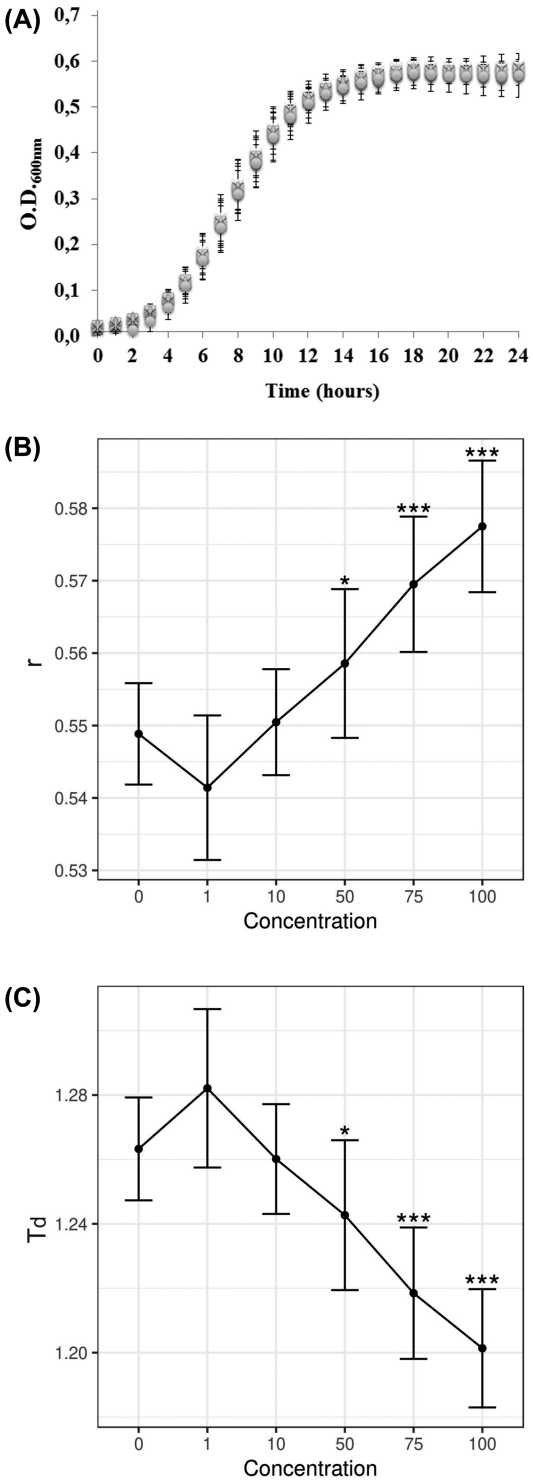

Figure 1. *Saccharomyces cerevisiae* BY4741 growth curves (A) with and without JWH-018 were fitted to the standard form of the logistic equation (Equation (1)), where *r* is the growth rate (B). The doubling time values (td) were computed from the growth rate using the formulae *Ln2/r* (C). These models showed to be significantly different from the null model for concentrations equal or higher than 50 μM of JWH-018 (* $P < 0.05$ or *** $P < 0.001$).

SC. Among them, seven spots show a decrease in protein levels, while one reveals an increase in protein level. Half of the spots are within basic or acidic regions of the isoelectric focusing gel strip. Besides, the remaining spots are within the most crowded region of the gel. Thus, the spots are in the working limits of the 2D-gel analysis (Rabilloud and Lelong 2011; Yaoita *et al.* 2014). To understand which proteins were changing in the presence of JWH-018, a table of soluble proteins matching the isoelectric point and molecular weight was generated for the eight spots under analysis using a list of all *S. cerevisiae* identified protein from UniProt database (https://www.uniprot.org) (UniProt Consortium 2019). The rationale for protein selection was based on the hypothesis that growth rate increment was due to expression changes in central metabolism enzymes and in protein production machinery. In the end, 15 proteins were selected and their mRNA expression was quantified by qRT-PCR, namely *ADH4*, *ADH5*, *EMI2*, *FBA1*, *GPM1*, *GPP1*, *NPY1*, *PGI1*, *PRM15*, *REE1*, *SER33*, *SOL3*, *SOL4*, *TAL1*, *ZWF1*. *PGK1* was used as control.

mRNA expression analysis

To further understand the changes in the proteome, the mRNA expression of *ADH4*, *ADH5*, *EMI2*, *FBA1*, *GPM1*, *GPP1*, *NPY1*, *PGI1*, *PRM15*, *REE1*, *SER33*, *SOL3*, *SOL4*, *TAL1*, *ZWF1* in the presence of JWH-018 was quantified by qRT-PCR. The concentration of JWH-018 chosen was 100μM, the same used in the 2D-Gel analysis. Three *S. cerevisiae* biological replicates were used both in the presence and absence of the drug. The results showed one gene upregulated, eight genes downregulated and five genes with no changes in mRNA expression after exposition to the SC (Fig. 4). The gene found upregulated in the presence of JWH-018 was *FBA1* (1.21). In contrast, the genes found downregulated were *ADH5* (0.87), *EMI2* (0.66), *NPY1* (0.77), *PRM15* (0.84), *REE1* (0.76), *SOL3* (0.87), *SOL4* (0.61) and *ZWF1* (0.70). The genes without differences in mRNA expression were *ADH4* (1.02), *GPP1* (0.99), *PGI1* (0.98), *SER33* (0.92) and *TAL1* (1.03). The statistical comparison between yeast mRNA expression in the absence and in the presence of JWH-018 showed six genes which present statistically significant differences, namely ADH5 ($P < 0.1$), *EMI2* ($P < 0.02$), FBA1 ($P < 0.02$), *SOL3* ($P < 0.1$), *SOL4* ($P < 0.02$) and *ZWF1* ($P < 0.05$) (Fig. 4). The mRNA results point an increase in the expression of several genes encoding glycolytic enzymes and a decreasing in the expression of the genes encoding enzymes from the oxidative phase of pentose phosphate pathway. These results suggest an increment in glycolytic pathway and a decrease in the pentose phosphate pathway flux (Fig. 4).

To further understand the relationship between these yeast enzymes, an *in silico* network of proteins was generated (Fig. 5). A network map of known protein–protein associations was obtained using STRING database for yeast proteins altered in response to JWH-018, as well as for the correspondent human orthologues (Fig. 5). This network includes interactions derived from functional associations (dos Santos *et al.* 2012). A higher number of interactions between the yeast enzymes identified were found with the yeast dataset. Most of the proteins are involved in glycolysis and gluconeogenesis pathways. In spite of all yeast proteins having a human counterpart, the interactions predicted for the human dataset are considerably less numerous, but still find a correspondence for the aforementioned pathways. It is noteworthy that the conservation of the yeast dataset in the human proteome and the analogies observed in the two biological systems implies that the results obtained in here may allow to gain insights into the molecular mechanisms of JWH-018 in human cells.

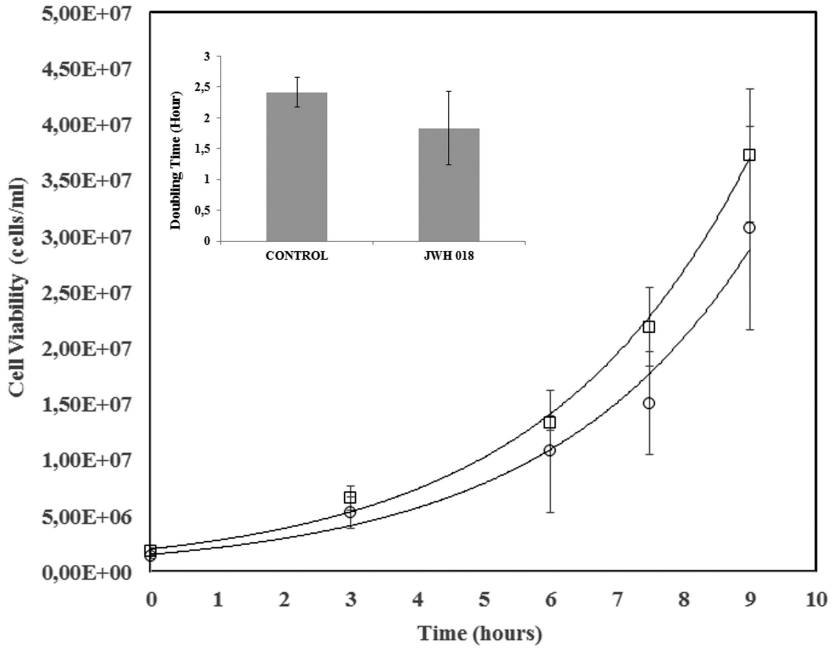

Figure 2. Exponential phase of *Saccharomyces cerevisiae* BY4741, in the absence (○) and presence of 50 μM of JWH-018 (□), determined by viable cell concentration, assessed as the number of CFU/mL of cell culture and its doubling time represented by the bar chart (the results are representative of at least three independent growth experiments).

ATP quantification

To confirm if the glycolytic pathway is upregulated in the presence of JWH-018, the ATP intracellular content was quantified on the different experimental conditions. Our results showed a decrease of 17.4% in ATP levels when *S. cerevisiae* was exposed to JWH-018 (Fig. 6). This decrease was shown to be significantly different from the culture without SC ($P < 0.001$).

DISCUSSION

To evaluate the cellular impact of JWH-018, yeast growth curves were used. The analysis of the growing curves showed an increase in cell growth rate, in the presence of the SC, which implies a decrease in duplication time when compared to the control. For concentration values of JWH-018 equal or higher than 50 μM, the increase in growth rate is significant ($P < 0.05$) suggesting a faster grow of yeast in the presence of this SC. To verify the outcomes of the previous analysis, a CFU assay was performed. Despite not statistically significant, the results indicate a decrease in yeast doubling time in the presence of 50 μM of JWH-018. Interestingly, a previous study with SH-SY5Y and HEK293T human cell lines showed that JWH-018 seems to increase cell viability, suggesting that yeast response to this SC is similar to human cell response (44). However, this study did not clarify the mechanims underlying JWH-018 effect on cellular growth.

To understand which proteins were involved in the increment of *S. cerevisiae* growth rate when in the presence of the SC, a proteomic study was conducted. 2D gel electrophoresis from soluble yeast proteome exposed to JWH-018 showed 2181 spots. The statistical comparative analysis of the gels in the absence and presence of 100 μM of the SC showed significative differences among eight spots. However, these spots were within basic or acidic regions of the isoelectric focusing gel strip or in the most crowded region of the gel limiting the identification of the spots. To overcome this problem, a bioinformatic analysis was performed to identify relevant proteins whose isoelectric points and molecular weights were in agreement with the spots that showed statistical differences. This approach showed 15 proteins whose genes expression was monitored by qRT-PCR.

The monitored genes are mostly related with the glycolytic and pentose phosphate pathways (Fig. 7). One of the genes under analysis was *EMI2* encoding a putative glucokinase-2 (EC:2.7.1.2) which is highly homologous to the glucokinase (EC:2.7.1.2). When expressed, this enzyme feeds both glycolysis and pentose phosphate pathway. However, *EMI2* is completely repressed by high concentrations of glucose and is expressed in the presence of moderate concentrations of glucose (Lutfiyya *et al.* 1998). The quantitative mRNA analysis of *EMI2* in the presence of JWH-018 showed a 50% decrease in its expression. This downregulation of *EMI2* suggests that yeast in the presence of JWH-018 wrongly perceives a higher amount of glucose in the medium.

Regarding the glycolytic pathway, the mRNA expression of *PGI1*, *FBA1*, *GPM1* and *REE1* was monitored. *PGI1* encodes phosphoglucose isomerase (EC:5.3.1.9), the first exclusive enzyme of glycolysis, which is responsible for the interconversion of glucose-6-phosphate to fructose-6-phosphate. *FBA1* encodes frutose-1,6-biphosphate aldolase (EC:4.1.2.13) which catalyses the reversible cleavage of fructose-1,6-bisphosphate to glyceraldehyde 3-phosphate and dihydroxyacetone phosphate (Cieśla *et al.* 2014). *GPM1* encodes phosphoglycerate mutase 1 (EC:5.4.2.11), a glycolytic enzyme responsible for the conversion of 3-phospholgycerate to 2-phosphoglycerate in glycolysis (Rodicio & Heinisch 1987; Smits *et al.* 2000; Price & Jaenicke 1982). Finally, *REE1* encodes Ree1, a cytoplasmatic protein involved in the negative regulation of Eno1 (EC:4.2.1.11). Eno1 catalyses the transformation of 2-phospoglycerate to phosphoenolpyruvate. Among these four genes, *PGI1* and *GPM2* showed no differences in mRNA expression, whereas *FBA1* ($P < 0.02$) showed an increase in mRNA expression and *REE1* showed a decrease in mRNA expression in the presence of the SC. Previous studies

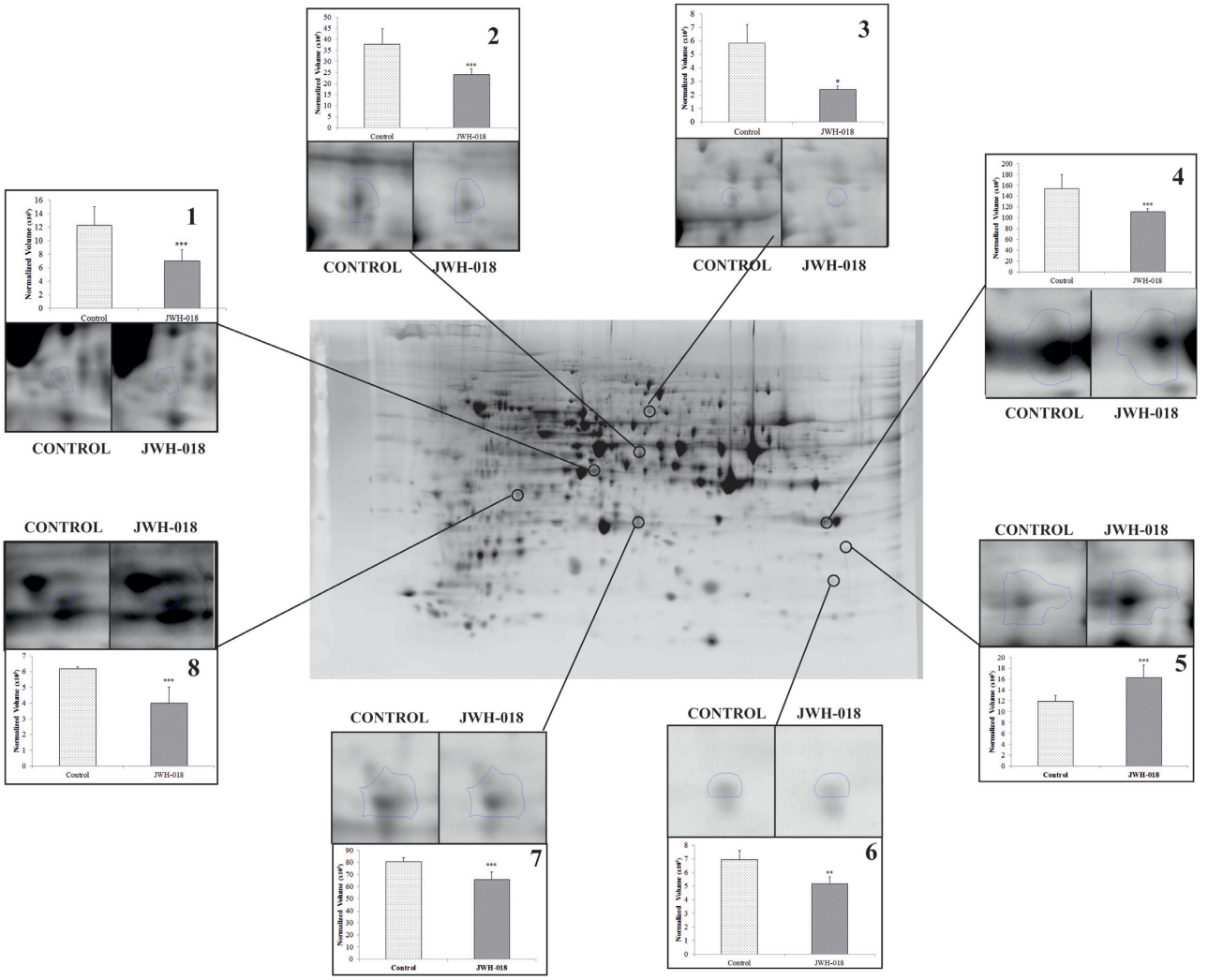

Figure 3. Proteome of *Saccharomyces cerevisiae* BY4741 in the presence of 100 μM of JWH-018. The proteome in the absence and in the presence of JWH-018 were analysed using Progenesis SameSpots (Totallab, UK). Throughout these comparisons triplicate 2D gels for each of the *S. cerevisiae* culture conditions were analysed. The range of protein separation obtained by a 2DE was 10–250 kDa and 3–10 pH and 2181 protein spots were detected through its analysis. Eight protein spots were found with statistically significant differences in their expression ($P < 0.05$).

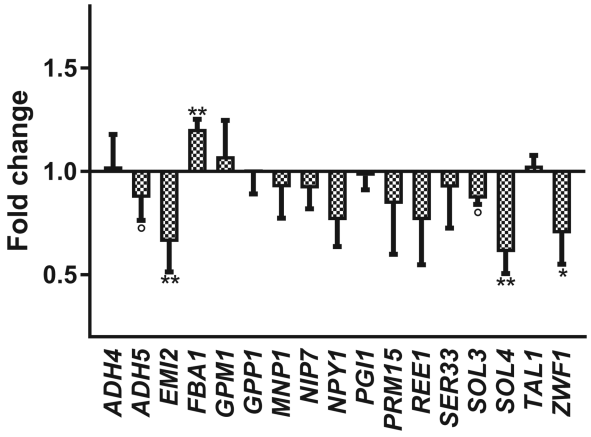

Figure 4. qRT-PCR showing relative changes of *S. cerevisiae* BY4741 in the presence of 100 μM of JWH-018. The results showed one gene upregulated, eight genes downregulated and six genes with no changes in mRNA expression after exposition to the SC. *PGK1* was used as control.

demonstrated that the increment in *FBA1* expression improves the glucose consumption rate (Wang *et al.* 2011). Consequently, an increment on *FBA1* expression points to an increase in yeast glycolytic flux when JWH-018 is present. Furthermore, the observed decrease in *REE1* expression reinforces the suggestion that glycolysis is upregulated by the SC, once Eno1 might be more active.

Additionally, four genes, indirectly related to glycolysis, were also studied, namely (i) *GPP1*, encoding a glycerol-3-phosphate phosphatase (EC 3.1.3.21), which is involved in glycerol biosynthesis (Norbeck *et al.* 1996), (ii) *SER33* which encodes a D-3-phosphoglycerate dehydrogenase 2 and is involved in the reversible oxidation of 3-phospho-D-glycerate to 3-phosphonooxypyruvate, the first step of the phosphorylated L-serine biosynthesis pathway (Albers *et al.* 2003), and (iii) *ADH4* and *ADH5* genes which encodes alcohol dehydrogenase 4 and 5 (1.1.1.1) respectively, and are involved in the interconversion between aldehydes and primary alcohols. The *GPP1*, *SER33* and *ADH4* mRNA expressions have not showed differences between control and 100 μM of JWH-018. *ADH5* ($P < 0.1$) mRNA expression is decreased in the presence of the SC. This decrease does not

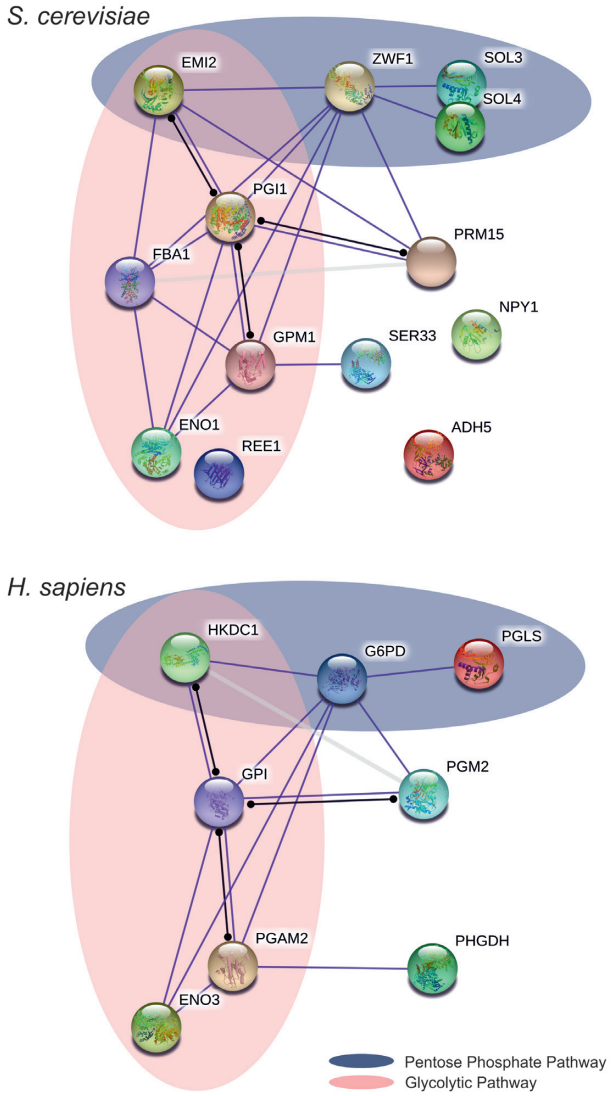

Figure 5. Protein interactions established with the entire JWH-018-responsive yeast protein dataset and in the corresponding dataset of human functional homologs. The protein interaction network maps shown were adapted from the output of STRING database tools, using the default parameters. The yeast proteins whose showed differences when compared to the control were submitted to obtain the *S. cerevisiae* map, whereas for the *Homo sapiens* map a few homologs were identified. All the yeast and human proteins indicated in the clusters are involved in glycolysis and pentose phosphate pathway.

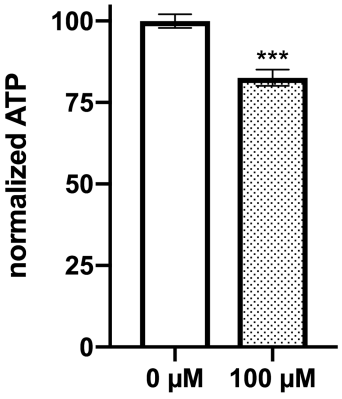

Figure 6. Intracellular ATP levels present in *S. cerevisiae* in the presence of 0 and 100 μM of JWH-018. The results showed a decrease in ATP levels in the presence of 100 μM of the SC ($P < 0.001$).

seem relevant once five different alcohol dehydrogenases are present in yeast cells.

Concerning the pentose phosphate pathway, the mRNA expression of *ZWF1*, *SOL3*, *SOL4* and *TAL1* was relatively quantified. *ZWF1* encodes glucose-6-phosphate dehydrogenase (EC:1.1.1.49) which catalyses the first step of the pentose phosphate pathway and competes with glycolysis for glucose 6-phosphate. When Zwf1 is not expressed, the pentose phosphate pathway is blocked (Jeppsson *et al.* 2002). *SOL3* and *SOL4* are paralogues genes encoding 6-phosphoglucolactonase 3 and 4 (EC:3.1.1.31) which catalysis the second step of pentose phosphate pathway (Stanford *et al.* 2004). In spite of the hydrolysis of the lactone ring is spontaneous, the lack of these enzymes decreases substantially the flux of the above-mentioned pathway (Yang *et al.* 2013). *PRM15* encodes the major phosphoribomutase (EC:5.4.2.7) that converts ribose 1-phosphate to ribose 5-phosphate in ribose salvage via the pentose phosphate pathway (Tiwari and Bhat 2008). Finally, *TAL1* encodes a transaldolase (EC:2.2.1.2) from the non-oxidative branch of pentose phosphate pathway which converts sedoheptulose 7-phosphate and glyceraldehyde 3-phosphate to erythrose 4-phosphate and fructose 6-phosphate (Schaaff, Hohmann and Zimmermann 1990). Among these five genes, *TAL1* showed no differences in mRNA expression, while *ZWF1* ($P < 0.05$), *SOL3* ($P < 0.1$), *SOL4* ($P < 0.02$) and *PRM15* showed a decrease in mRNA expression in the presence of the JWH-018. The significative decrease in mRNA expression of *ZWF1*, *SOL3* and *SOL4* mRNA clearly points to a reduction in the flux of glucose-6-phosphate in the oxidative branch of pentose phosphate pathway. Moreover, the decrease in *PRM15* mRNA expression suggests a tendency to reduce the transformation of ribose-5-phosphate to ribose-1-phosphate, diminishing the outflux of ribose-5-phosphate from the pentose phosphate pathway.

Lastly, mRNA expression of *NPY1*, a gene not directly associated with glycolysis and pentose phosphate pathway, was also monitored. *NPY1* encodes a diphosphatase (pyrophosphatase) (EC:3.6.1.22) with NADH as the preferred substrate, originating NMNH and AMP as products (AbdelRaheim *et al.* 2001). *NPY1* mRNA expression is decreased in the presence of JWH-018. Once NAD^+ is essential for glyceraldehyde 3-P dehydrogenase phosphorylative oxidation, a key step in glycolysis, the results suggest that decreasing NAD^+ turnover might turn this molecule more available to anaerobic glucose consumptions.

In general, metabolic pathways are controlled by regulation of enzymes activity and variation in their amount. For example, the flux of glucose-6-phosphate through the pentose-phosphate pathway in yeast cells is controlled by variation in the amounts of glucose-6-phosphate dehydrogenase (Yang *et al.* 2013). The mRNA expression results suggest the increase in Fba1 and Gpm1 in glycolysis and the decrease in Zwf1, Sol3 and Sol4 in pentose phosphate pathway. These data support that JWH-018 increases the flux of glucose through glycolysis at expenses of pentose phosphate pathway (Fig. 7). Such metabolic shift might reduces NADPH available to cytochrome P450 used in phase I metabolism SC. However, yeast has not homologous of the cytochromes P450 which metabolized JWH-018 in humans, namely CYP1A2 and 2C9 (Chimalakonda *et al.* 2012).

An increase of glycolysis should be combined with a change in ATP levels. In fact, there is a strong negative correlation between glycolytic flux and intracellular ATP content, meaning that the lower the ATP content the higher the rate of glycolysis (Lagunas 1976; Larsson *et al.* 1997; Somsen *et al.* 2000; Özalp *et al.* 2010). To corroborate the upregulation of glycolysis by JWH-018 an ATP measurement of yeast cells in the presence and absence

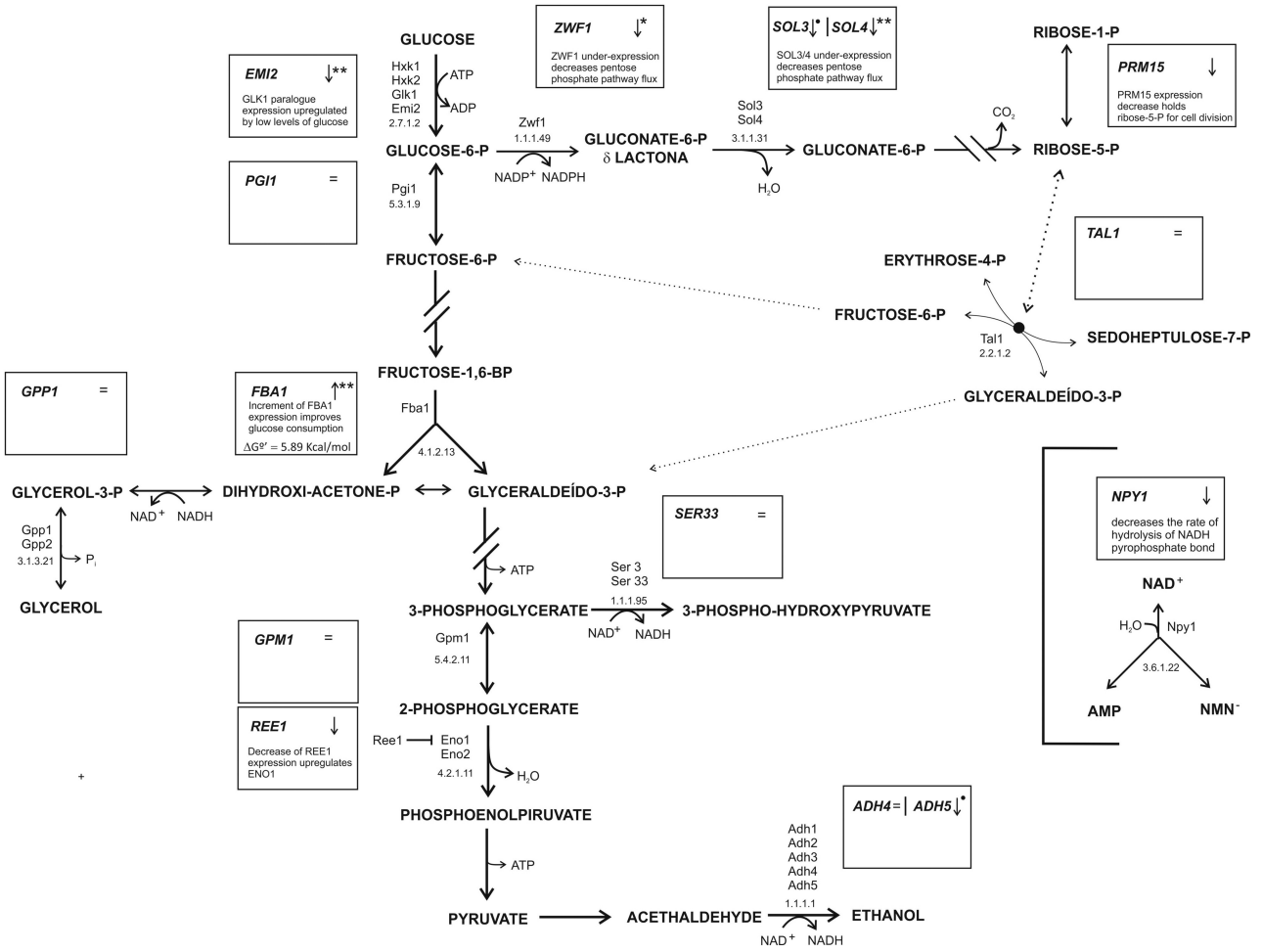

Figure 7. Representation of genes, enzymes and intermediates from glycolysis, pentose phosphate pathways and associated off-pathways in *S. cerevisiae*. The scheme shows the differences in gene expression from *ADH4*, *ADH5*, *EMI2*, *FBA1*, *GPM1*, *GPP1*, *NPY1*, *PGI1*, *PRM15*, *REE1*, *SER33*, *SOL3*, *SOL4*, *TAL1*, *ZWF1* in the presence of JWH-018.

of the SC was taken. The results showed a decrease of 17.4% in ATP yeast levels in the presence of this SC, confirming an upregulation of glycolysis.

Overall, the results strongly suggest that the SC JWH-018 promotes cellular growth by modulating protein levels of glycolytic and pentose phosphate enzymes. Moreover, the conservation of the yeast dataset in the human proteome and the analogies observed in the two biological systems implies that the results obtained in here may allow to gain insights into the molecular mechanisms of JWH-018 in human cells.

CONCLUSION

Previous studies showed that JWH-018 increases human neuroblastoma cells viability (Couceiro *et al.* 2016). The present work observed an increase in the growth rate of *S. cerevisiae* exposed to the same compound, in line with the above-mentioned results. However, the underlying mechanisms of this effect was not clarified before. In fact, since the appearance of JWH-018 in the headshops for recreational use, ten years ago, there are no published studies explaining the metabolic changes associated to the increase in cellular growth. The results in this study showed that the increase in *S. cerevisiae* growth rate, in the presence of JWH-018, is due to an enhanced glycolytic flux at expense of a decrease in pentose phosphate pathway. The present work implements *S. cerevisiae* as a model to better understand SC at fundamental molecular and cellular levels, allowing to design oriented studies in human cells or animal models. Along with recent studies on synthetic cathinones, yeast has been revealing an excellent model to study novel psychoactive substances (Ferreira *et al.* 2019).

SUPPLEMENTARY DATA

Supplementary data are available at *FEMSYR* online.

ACKNOWLEDGEMENTS

This work was funded by Egas Moniz, Cooperativa de Ensino Superior. We thank its unconditional support. TFO is supported by the DFG Center for Nanoscale Microscopy and Molecular Physiology of the Brain (CNMPB).

CNS and ST also acknowledge Fundação para a Ciência e Tecnologia financial support (IF/01097/2013 and SFRH/BPD/101646/2014, respectively) iNOVA4Health Research Unit (LISBOA-01–0145-FEDER-007344), which is cofounded by FCT through national funds, and by FEDER under the PT2020 Partnership Agreement, is acknowledged. The Forensic and

Psychological Sciences Laboratory has a license to possess and use, for scientific purposes, drugs of abuse. The authors declare no conflict of interest.

Conflict of interest. None declared.

REFERENCES

AbdelRaheim SR, Cartwright JL, Gasmi L *et al.* The NADH Diphosphatase encoded by the Saccharomyces cerevisiae NPY1 nudix hydrolase gene is located in peroxisomes. *Arch Biochem Biophys* 2001;**388**:18–24.

Albers E, Laizé V, Blomberg A *et al.* Ser3p (Yer081wp) and Ser33p (Yil074cp) are phosphoglycerate dehydrogenases in saccharomyces cerevisiae. *J Biol Chem* 2003;**278**:10264–72.

Askew WE, Ho BT. Effects of tetrahydrocannabinols on cyclic AMP levels in rat brain areas. *Experientia* 1974;**30**:879–80.

Bar-Joseph A, Berkovitch Y, Adamchik J *et al.* Neuroprotective activity of HU-211, a novel NMDA antagonist, in global ischemia in gerbils. *Mol Chem Neuropathol* 1994;**23**: 125–35.

Chimalakonda KC, Seely KA, Bratton SM *et al.* Cytochrome P450-mediated oxidative metabolism of abused synthetic cannabinoids found in K2/Spice: Identification of novel cannabinoid receptor ligands. *Drug Metab Dispos* 2012;**40**:2174–84.

Cieśla M, Mierzejewska J, Adamczyk Met al. Fructose biphosphate aldolase is involved in the control of RNA polymerase III-directed transcription . *Biochim Biophys Acta* 2014; **1843** :1103–10 .

Clifford DB. Tetrahydrocannabinol for tremor in multiple sclerosis. *Ann Neurol* 1983;**13**:669–71.

Couceiro J, Bandarra S, Sultan H *et al.* Toxicological impact of JWH-018 and its phase I metabolite N-(3-hydroxypentyl) on human cell lines. *Forensic Sci Int* 2016;**264**:100–5.

Crane EH, in *Highlights of the 2011 Drug Abuse Warning Network (DAWN) findings on drug-related emergency department visits*, **2011**, (The CBHSQ Report, 2013), 1–8.

Devane WA, Dysarz FA, Johnson MR *et al.* Determination and characterization of a cannabinoid receptor in rat brain. *Mol Pharmacol* 1988;**34**:605–13.

dos Santos SC, Mira NP, Moreira AS *et al.* Quantitative- and phospho-proteomic analysis of the yeast response to the tyrosine kinase inhibitor imatinib to pharmacoproteomics-guided drug line extension. *Omi A J Integr Biol* 2012;**16**:120709112953007.

Fantegrossi WE, Wilson CD, Berquist MD. Pro-psychotic effects of synthetic cannabinoids: Interactions with central dopamine, serotonin, and glutamate systems. *Drug Metab Rev* 2018;**50**:65–73.

Fernández-López D, Martínez-Orgado J, Nuñez E *et al.* Characterization of the neuroprotective effect of the cannabinoid agonist WIN-55212 in an In Vitro model of hypoxic-ischemic brain damage in newborn rats. *Pediatr Res* 2006;**60**:169–73.

Ferreira C, Vaz AR, Florindo PR *et al.* Development of a high throughput methodology to screen cathinones' toxicological impact. *Forensic Sci Int* 2019;**298**:1–9.

Gaoni Y, Mechoulam R. Isolation, structure, and partial synthesis of an active constituent of Hashish. *J Am Chem Soc* 1964;**86**:1646–7.

Gruol DL, Sweeney DD, Conroy SM *et al.* Cannabinoids alter neurotoxicity produced by Interleukin-6 in central nervous system neurons. *Adv Exp Med Biol* 1998;**437**:231–40.

Heepe P, Starke K. Alpha-adrenoceptor antagonists and the release of noradrenaline in rabbit cerebral cortex slices: Support for the alpha-autoreceptor hypothesis. *Br J Pharmacol* 1985;**84**:147–55.

Howlett AC, Barth F, Bonner TI *et al.* International union of pharmacology. XXVII. Classification of cannabinoid receptors. *Pharmacol Rev* 2002;**54**:161–202.

Howlett AC, Qualy JM, Khachatrian LL. Involvement of Gi in the inhibition of adenylate cyclase by cannabimimetic drugs. *Mol Pharmacol* 1986;**29**:307–13.

Hu Y, Wang G, Chen GYJ *et al.* Proteome analysis of Saccharomyces cerevisiae under metal stress by two-dimensional differential gel electrophoresis. *Electrophoresis* 2003;**24**:1458–70.

Irie T, Kikura-Hanajiri R, Usami M *et al.* MAM-2201, a synthetic cannabinoid drug of abuse, suppresses the synaptic input to cerebellar Purkinje cells via activation of presynaptic CB1 receptors. *Neuropharmacology* 2015;**95**:479–91.

Jeppsson M, Johansson B, Hahn-Hägerdal Bet al. Reduced oxidative pentose phosphate pathway flux in recombinant xylose-utilizing Saccharomyces cerevisiae strains improves the ethanol yield from xylose. *Appl Environ Microbiol* 2002;**68**:1604–9.

Koch M, Kreutz S, Böttger C *et al.* The cannabinoid WIN 55,212-2-mediated protection of dentate gyrus granule cells is driven by CB1 receptors and modulated by TRPA1 and Cav2.2 channels. *Hippocampus* 2011;**21**:554–64.

Koller VJ, Zlabinger GJ, Auwärter V *et al.* Toxicological profiles of selected synthetic cannabinoids showing high binding affinities to the cannabinoid receptor subtype CB1. *Arch Toxicol* 2013;**87**:1287–97.

Lagunas R. Energy metabolism of Saccharomyces cerevisiae discrepancy between ATP balance and known metabolic functions. *Biochim Biophys Acta - Bioenerg* 1976;**440**: 661–74.

Lainton JAH, Huffman JW, Martin BR *et al.* 1-Alkyl-3-(1-naphthoyl) pyrroles: A new class of cannabinoid. *Tetrahedron Lett* 1995;**36**:1401–4.

Larsson C, Nilsson A, Blomberg A *et al.* Glycolytic flux is conditionally correlated with ATP concentration in. *Microbiology* 1997;**179**:7243–50.

Lee SL, Phillis JW. Stimulation of cerebral cortical synaptosomal Na-K-ATPase by biogenic amines. *Can J Physiol Pharmacol* 1977;**55**:961–4.

Li DM, Ng CK. Effects of delta 1- and delta 6-tetrahydrocannabinol on the adenylate cyclase activity in ventricular tissue of the rat heart. *Clin Exp Pharmacol Physiol* 1984;**11**:81–5.

Lutfiyya LL, Iyer VR, DeRisi Jet al. Characterization of three related glucose repressors and genes they regulate in Saccharomyces cerevisiae. *Genetics* 1998;**150**:1377–91.

Malyshevskaya O, Aritake K, Kaushik MK *et al.* Natural (Δ9-THC) and synthetic (JWH-018) cannabinoids induce seizures by acting through the cannabinoid CB1 receptor. *Sci Rep* 2017;**7**:10516.

McCarthy LE, Borison HL. Antiemetic activity of N-methyllevonantradol and nabilone in cisplatin-treated cats. *J Clin Pharmacol* 1981;**21**:30S–37S.

Meijer KA, Russo RR, Adhvaryu DV. Smoking synthetic marijuana leads to self-mutilation requiring bilateral amputations. *Orthopedics* 2014;**37**:e391–4.

Nagayama T, Sinor AD, Simon RP *et al.* Cannabinoids and neuroprotection in global and focal cerebral ischemia and in neuronal cultures. *J Neurosci* 1999;**19**:2987–95.

Norbeck J, Pâhlman AK, Akhtar N *et al.* Purification and characterization of two isoenzymes of DL-glycerol-3-phosphatase from Saccharomyces cerevisiae. Identification of the corresponding GPP1 and GPP2 genes and evidence for osmotic regulation of Gpp2p expression by the osmosensing mitogenacti. *J Biol Chem* 1996;**271**:13875–81.

Nurmedov S, Metin B, Ekmen S *et al.* Thalamic and cerebellar gray matter volume reduction in synthetic cannabinoids users. *Eur Addict Res* 2015;**21**:315–20.

Petro DJ, Ellenberger C. Treatment of human spasticity with delta 9-tetrahydrocannabinol. *J Clin Pharmacol* 1981;**21**:413S–416S.

Pinar-Sueiro S, Zorrilla Hurtado JÁ, Veiga-Crespo P *et al.* Neuroprotective effects of topical CB1 agonist WIN 55212-2 on retinal ganglion cells after acute rise in intraocular pressure induced ischemia in rat. *Exp Eye Res* 2013;**110**: 55–8.

Price NC, Jaenicke R. The quaternary structure of phosphoglycerate mutase from yeast against dissociation of the tetrameric enzyme at low concentrations. *FEBS Lett* 1982;**143**:283–6.

Puffenbarger RA, Boothe AC, Cabral GA. Cannabinoids inhibit LPS-inducible cytokine mRNA expression in rat microglial cells. *Glia* 2000;**29**:58–69.

Qamri Z, Preet A, Nasser MW *et al.* Synthetic cannabinoid receptor agonists inhibit tumor growth and metastasis of breast cancer. *Mol Cancer Ther* 2009;**8**:3117–29.

Rabilloud T, Lelong C. Two-dimensional gel electrophoresis in proteomics: A tutorial. *J Proteomics* 2011;**74**:1829–41.

Reich R, Laufer N, Lewysohn O *et al.* In vitro effects of cannabinoids on follicular function in the rat. *Biol Reprod* 1982;**27**:223–31.

Robinson L, Goonawardena AV, Pertwee RG *et al.* The synthetic cannabinoid HU210 induces spatial memory deficits and suppresses hippocampal firing rate in rats. *Br J Pharmacol* 2007;**151**:688–700.

Rodicio R, Heinisch J. Isolation of the yeast phosphoglyceromutase gene ans construction of deletion mutants. *Mol Gen Genet* 1987;**206**:133–40.

Rojek SD, Korczyńska-Albert M, Kulikowska J *et al.* New challenges in toxicology of new psychoactive substances exemplified by fatal cases after UR-144 and UR-144 with pentedrone administration determined by LC-ESI-MS-MS in blood samples. *Arch Forensic Med Criminol* 2017;**2**: 104–20.

Schaaff I, Hohmann S, Zimmermann FK. Molecular analysis of the structural gene for yeast transaldolase. *Eur J Biochem* 1990;**188**:597–603.

Schmitt M, Gellert G, Ludwig J *et al.* Phenotypic yeast growth analysis for chronic toxicity testing. *Ecotoxicol Environ Saf* 2004;**59**:142–50.

Shen M, Thayer SA. Cannabinoid receptor agonists protect cultured rat hippocampal neurons from excitotoxicity. *Mol Pharmacol* 1998;**54**:459–62.

Shohami E, Gallily R, Mechoulam R *et al.* Cytokine production in the brain following closed head injury: Dexanabinol (HU-211) is a novel TNF-α inhibitor and an effective neuroprotectant. *J Neuroimmunol* 1997;**72**:169–77.

Shohami E, Novikov M, Mechoulam R. A nonpsychotropic cannabinoid, HU-211, has cerebroprotective effects after closed head injury in the rat. *J Neurotrauma* 1993;**10**:109–19.

Smith SR, Terminelli C, Denhardt G. Effects of cannabinoid receptor agonist and antagonist ligands on production of inflammatory cytokines and anti-inflammatory interleukin-10 in endotoxemic mice. *J Pharmacol Exp Ther* 2000;**293**:136–50.

Somsen OJG, Hoeben MA, Esgalhado E *et al.* Glucose and the ATP paradox in yeast. *Biochem J* 2000;**352**:593–9.

Stanford DR, Whitney ML, Hurto RLet al. Division of labor among the yeast Sol proteins implicated in tRNA nuclear export and carbohydrate metabolism. *Genetics* 2004;**168**:117–27.

Tenreiro S, Munder MC, Alberti S *et al.* Harnessing the power of yeast to unravel the molecular basis of neurodegeneration. *J Neurochem* 2013;**127**:438–52.

Tenreiro S, Outeiro TF. Simple is good: Yeast models of neurodegeneration. *FEMS Yeast Res* 2010;**10**:970–9.

Theunissen EL, Hutten NRPW, Mason NL *et al.* Neurocognition and subjective experience following acute doses of the synthetic cannabinoid JWH-018: A phase 1, placebo-controlled, pilot study. *Br J Pharmacol* 2018;**175**:18–28.

Tiwari A, Bhat J. Molecular characterization reveals that YMR278w encoded protein is environmental stress response homologue of Saccharomyces cerevisiae PGM2. *Biochem Biophys Res Commum* 2008;**366**:340–5.

UniProt Consortium. UniProt: A worldwide hub of protein knowledge. *Nucl Acids Res* 2019;**47**:D506–15.

Urits I, Borchart M, Hasegawa M *et al.* An update of current cannabis-based pharmaceuticals in pain medicine. *Pain Ther* 2019;**8**:41–51. DOI: 10.1007/s40122-019-0114-4.

Vered M, Bar-Joseph A, Belayev L *et al.* Anti-ischemia activity of HU-211, a non-psychotropic synthetic cannabinoid. In: Ito U, Baethmann A, Hossmann K-A *et al.* (eds). *Brain Edema IX*. Vienna: Springer Vienna, 1994, 335–7.

von Mering C, Jensen LJ, Kuhn M *et al.* STRING 7–recent developments in the integration and prediction of protein interactions. *Nucl Acids Res* 2007;**35**:D358–62.

Wang S, Spor A, Nidelet Tet al. Switch between life history strategies due to changes in glycolitic enzyme gene dosage in Saccharomyces cerevisiae. *Appl Environ Microbiol* 2011;**77**:452–9.

Wiley JL, Compton DR, Dai D *et al.* Structure-activity relationships of indole- and pyrrole-derived cannabinoids. *J Pharmacol Exp Ther* 1998;**285**:995–1004.

Yang C, Xue X-S, Jin J-L *et al.* Theoretical study on the acidities of chiral phosphoric acids in dimethyl sulfoxide: Hints for organocatalysis. *J Org Chem* 2013;**78**:7076–85.

Yaoita E, Magdeldin S, Yoshida Y *et al.* Basics and recent advances of two dimensional- polyacrylamide gel electrophoresis. *Clin Proteomics* 2014;**11**:16.

Zuardi AW. History of cannabis as a medicine: A review. *Rev Bras Psychiatr* 2006;**28**:153–7.

Özalp VC, Pedersen TR, Nielsen LJ *et al.* Time-resolved measurements of intracellular ATP in the yeast saccharomyces cerevisiae using a new type of nanobiosensor. *J Biol Chem* 2010;**285**:37579–88.